

# Measurement of the neutron timelike electric and magnetic form factors ratio at the VEPP-2000 $e^+e^-$ collider

M. N. Achasov,<sup>1,2</sup> A. E. Alizzi,<sup>1,2</sup> A. Yu. Barnyakov,<sup>1,2</sup> E. V. Bedarev,<sup>1,2</sup> K. I. Beloborodov,<sup>1,2</sup> A. V. Berdyugin,<sup>1,2</sup> A. G. Bogdanchikov,<sup>1</sup> A. A. Botor,<sup>1</sup> T. V. Dimova,<sup>1,2</sup> V. P. Druzhinin,<sup>1,2</sup> R. A. Efremov,<sup>1</sup> V. N. Zhabin,<sup>1,2</sup> V. V. Zhulanov,<sup>1</sup> P. V. Zhulanova,<sup>1</sup> L. V. Kardapoltsev,<sup>1,2</sup> A. S. Kasaev,<sup>1</sup> A. A. Kattsin,<sup>1</sup> D. P. Kovrizhin,<sup>1</sup> I. A. Koop,<sup>1,2</sup> A. A. Korol,<sup>1,2</sup> A. S. Kupich,<sup>1,2</sup> A. P. Kryukov,<sup>1</sup> N. A. Melnikova,<sup>1</sup> N. Yu. Muchnoi,<sup>1,2</sup> A. E. Obrazovsky,<sup>1</sup> A. A. Oorzhak,<sup>1,2</sup> I. V. Ovtin,<sup>1</sup> E. V. Pakhtusova,<sup>1</sup> I. A. Polomoshnov,<sup>1</sup> K. V. Pugachev,<sup>1,2</sup> S. A. Rastigeev,<sup>1</sup> Yu. A. Rogovsky,<sup>1,2</sup> A. I. Senchenko,<sup>1</sup> S. I. Serednyakov,<sup>1,2,\*</sup> Z. K. Silagadze,<sup>1,2</sup> K. D. Sungurov,<sup>1,2</sup> I. K. Surin,<sup>1</sup> Yu. V. Usov,<sup>1</sup> A. G. Kharlamov,<sup>1,2</sup> D. E. Chistyakov,<sup>1,2</sup> and D. A. Shtol<sup>1</sup>

<sup>1</sup>Budker Institute of Nuclear Physics, SB RAS, Novosibirsk 630090, Russia

<sup>2</sup>Novosibirsk State University, Novosibirsk 630090, Russia

(Dated: )

In the experiment to study the  $e^+e^- \rightarrow n\bar{n}$  process at the VEPP-2000  $e^+e^-$  collider, the ratio  $|G_E|/|G_M|$  of the neutron timelike electric and magnetic form factors has been measured. The experiment was carried out with the SND detector in the center-of-mass energy range 1890–2000 MeV in 8 energy points with an integrated luminosity of  $83 \text{ pb}^{-1}$ . The  $|G_E|/|G_M|$  ratio is determined by the analyzing the distribution of the polar angle of the produced antineutron. The measured  $|G_E|/|G_M|$  value in the energy range under study is between 1.0 and 1.5 with an average value of  $1.21 \pm 0.13$ .

## Introduction

The most important parameters of nucleons are their electromagnetic form factors, determined by their interaction with photons. In  $e^+e^-$  annihilation the process of neutron-antineutron pair production

$$e^+e^- \rightarrow n\bar{n} \quad (1)$$

occurs through a virtual photon. Its cross section depends on two form factors, electric ( $G_E$ ) and magnetic ( $G_M$ ):

$$\frac{d\sigma}{d\Omega} = \frac{\alpha^2 \beta}{4s} \left[ |G_M(s)|^2 (1 + \cos^2 \theta) + \frac{1}{\gamma^2} |G_E(s)|^2 \sin^2 \theta \right], \quad (2)$$

where  $\alpha$  is the fine structure constant,  $s = 4E_b^2 = E^2$ , where  $E_b$  is the beam energy and  $E = 2E_b$  is the center-of-mass (c.m.) energy,  $\beta = \sqrt{1 - 4m_n^2/s}$ ,  $\gamma = E_b/m_n$ ,  $m_n$  is the neutron mass, and  $\theta$  is the antineutron production polar angle.

The total cross section has the following form:

$$\sigma(s) = \frac{4\pi\alpha^2\beta}{3s} \left( 1 + \frac{1}{2\gamma^2} \right) |F(s)|^2, \quad (3)$$

where the effective form factor  $F(s)$  is introduced:

$$|F(s)|^2 = \frac{2\gamma^2 |G_M(s)|^2 + |G_E(s)|^2}{2\gamma^2 + 1}. \quad (4)$$

The effective form factor  $|F(s)|^2$  shows the difference between the total cross section (3) and the cross section for pointlike nucleons, for which  $|F(s)|^2 = 1$ . There is an additional condition  $|G_E| = |G_M|$  at the threshold.

The  $e^+e^- \rightarrow n\bar{n}$  process was first observed in the FENICE [1] experiment. Recent measurements of this process were carried out at the VEPP-2000 collider with the SND detector at c.m. energies from the very threshold up to 2 GeV [2–5]. At energies above 2 GeV, cross section data were obtained by the BESIII [6]. In this work we present the SND results on the  $|G_E|/|G_M|$  ratio measurements in the energy range 1890–2000 MeV.

## I. COLLIDER, DETECTOR, EXPERIMENT

The VEPP-2000  $e^+e^-$  collider [7] has been operating since year 2011. It covers the energy range from the hadron production threshold E=280 MeV to 2 GeV. The collider luminosity depends on energy and is about  $5 \times 10^{31} \text{ cm}^{-2}\text{s}^{-1}$  above the nucleon threshold. There are two beam collision areas at VEPP-2000, one of which is occupied by the SND detector.

The SND detector [8] (Fig.1) and its operation in  $n\bar{n}$  experiments are described in previous publications [2–4]. Its main part is a well segmented ( $\Delta\phi = \Delta\theta = 9^\circ$ ) NaI(Tl) calorimeter (EMC). The calorimeter thickness of 35 cm NaI(Tl) is sufficient to absorb neutrons and antineutrons from the process (1). The calorimeter is equipped with the time measurement system [9] to measure event time relative to the beam collision time. The system time resolution measured for the  $e^+e^- \rightarrow \gamma\gamma$  events is 0.8 ns. This system plays an important role in identifying the time delayed  $n\bar{n}$  events. The internal

\*Electronic address: S.I.Serednyakov@inp.nsk.su

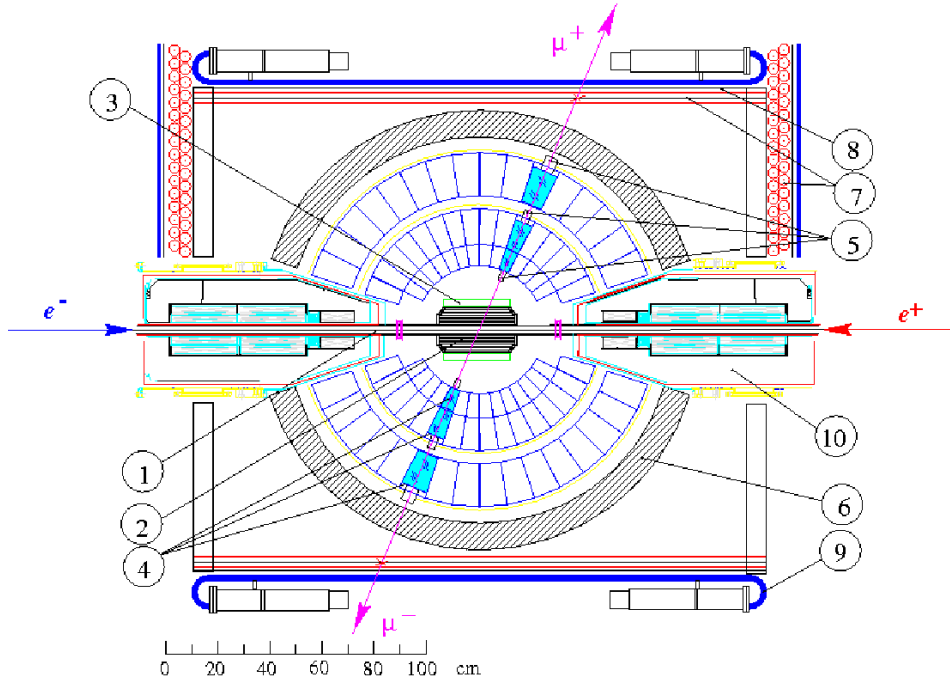


FIG. 1: SND detector, section along the beams: (1) beam pipe, (2) tracking system, (3) aerogel Cherenkov counters, (4) NaI (Tl) crystals, (5) vacuum photodiodes, (6) iron absorber, (7) proportional tubes, (8) iron absorber, (9) scintillation counters, (10) VEPP-2000 focusing solenoids.

tracking system is used in anticoincidence in this analysis to suppress the beam background. The external system (proportional tubes and scintillation counters), located outside the EMC and the iron absorber, is used to suppress the cosmic-ray background.

The data were collected at eight energy points in the 1890–2007 MeV range. They are listed in Table I. The total integrated luminosity is  $83 \text{ pb}^{-1}$ . The  $e^+e^- \rightarrow n\bar{n}$  cross section in this experiment was measured in Ref. [4]. In this work, we measure the neutron  $|G_E|/|G_M|$  ratio.

## II. EVENT SELECTION

Antineutrons from the process 1 annihilate in EMC, giving a large signal of up to 2 GeV. The signal from the accompanying neutron is comparatively weak and is not used. The antineutron polar angle  $\theta$ , used in our analysis, is defined by the direction of the total event momentum  $P_{EMC} = \sum_i E_i n_i$ , where the summation is carried out over the triggered EMC crystals,  $E_i$  is the crystal energy deposition,  $n_i$  is its position unit vector. Projections of the vector  $P_{EMC}$  onto the direction along and across the beams define the polar and azimuthal antineutron angles.

The selection criteria for  $n\bar{n}$  events were developed in our previous works [2–5]. The main conditions are following:

1. no charged tracks in the tracking system;
2. veto signal from the external system;

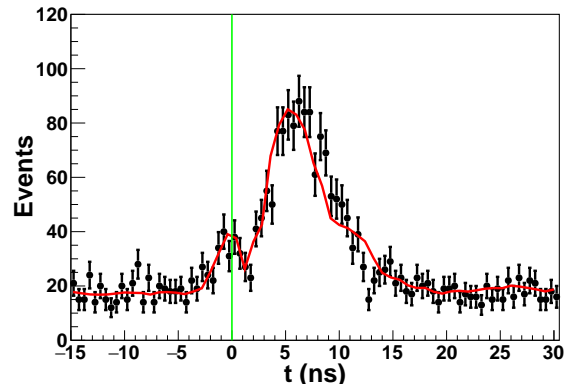


FIG. 2: The time distribution for selected data events at  $E_b = 950 \text{ MeV}$  (points with error bars). The wide peak to the right is formed by delayed  $n\bar{n}$  events. The vertical line at  $t = 0$  shows the time of beam collision. The red curve is the fit of the time spectrum described in the text.

3. no cosmic track or shower in EMC;
4. large event momentum imbalance in EMC  $P_{EMC} > 0.4E_b$ ;
5. large transverse EMC energy profile [10];
6. high total energy deposition in EMC  $E_{EMC} > E_b$ .

After applying the selection criteria, approximately  $400 \text{ events/pb}^{-1}$  remain for further analysis. The re-

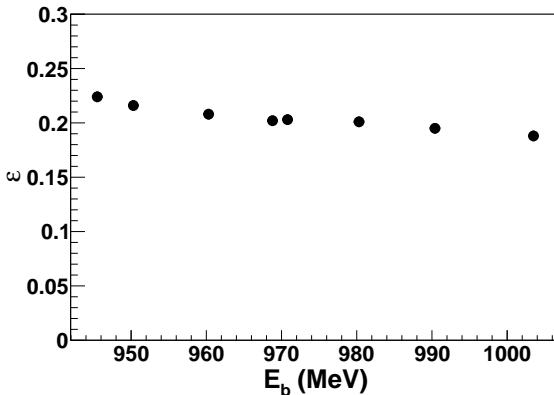


FIG. 3: The MC detection efficiency  $\varepsilon$  for  $e^+e^- \rightarrow n\bar{n}$  process versus the beam energy.

maining events are divided into three types, depending on their time distribution relative to the moment of the beam collision ( $t=0$ ): the cosmic-ray events, uniformly distributed in time; the beam-induced and physical background events concentrated around zero time, and  $n\bar{n}$  events shifted relative to zero time by  $\sim 10$  ns. An example of the time spectrum for selected events is shown in Fig. 2, where these three types of events are visible. It is seen that the measured spectrum for  $n\bar{n}$  events is quite wide in time due to the spread of the antineutron annihilation point inside the calorimeter. To obtain the number of  $n\bar{n}$  and background events, the measured time spectra at each energy point are fitted by the sum of three mentioned above contributions in the following form :

$$F(t) = N_{n\bar{n}} H_{n\bar{n}}(t) + N_{\text{cosm}} H_{\text{cosm}}(t) + N_{\text{bkg}} H_{\text{bkg}}(t), \quad (5)$$

where  $H_{\text{cosm}}$  and  $H_{\text{bkg}}$  are the cosmic-ray and beam background time spectra, measured at energy below the  $n\bar{n}$  threshold,  $H_{n\bar{n}}$  is the Monte-Carlo (MC) simulated  $n\bar{n}$  time spectrum [11],  $N_{n\bar{n}}$ ,  $N_{\text{cosm}}$ , and  $N_{\text{bkg}}$  are the event numbers for the three contributions. The fitted numbers of  $n\bar{n}$  events and other data on the experiment are listed in Table I.

The MC detection efficiency, obtained using the selection criteria described above, is about 20%. It is shown in Fig. 3 as a function of the beam energy and in Fig. 4 as a function of the cosine of the antineutron polar angle ( $\cos \theta$ ) at the beam energy 980 MeV.

### III. DISTRIBUTION OF $\cos \theta$

To obtain experimental  $\cos \theta$  distribution, we divide the  $-0.9 < \cos \theta < 0.9$  range into 18 intervals. In each  $\cos \theta$  interval the fit to the time spectrum is performed as is described in Sec. II and the number of  $n\bar{n}$  events is determined. The obtained  $\cos \theta$  distribution at  $E_b = 970$  MeV is shown in Fig. 5. The bins with  $|\cos \theta| =$

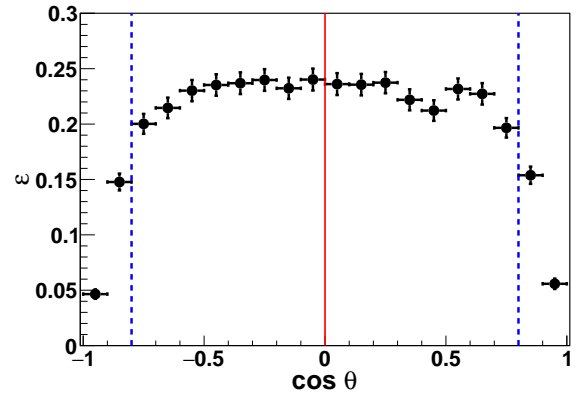


FIG. 4: The MC detection efficiency  $\varepsilon$  versus  $\cos \theta$ . The vertical lines at  $\cos \theta = \pm 0.8$  show the area used in analysis.

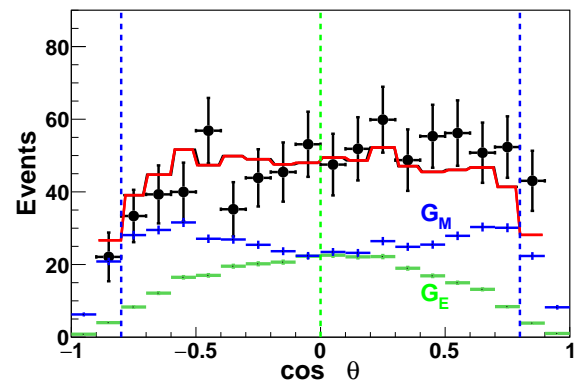


FIG. 5: The  $\cos \theta$  distribution of selected  $n\bar{n}$  events at the beam energy 970 MeV (points with error bars). The solid (red) curve is the result of the fit described in the text. The histograms labeled  $G_E$  and  $G_M$  show the contributions of the electric and magnetic form factors, respectively. The vertical lines at  $\cos \theta = \pm 0.8$  delimit the area for analysis.

0.8–0.9 correspond to the edge of the sensitive area of the calorimeter. Thus, the main  $\cos \theta$  interval, used in the subsequent analysis, lies within  $-0.8$ – $0.8$ .

When studying the data  $\cos \theta$  distributions, a right/left asymmetry was unexpectedly revealed in these spectra. It is most clearly seen in the distribution at  $E_b = 970$  MeV shown in Fig. 5. Since the measured angle  $\theta$  corresponds to the antineutron angle, the right/left asymmetry is also a charge asymmetry. The asymmetry  $\alpha_{as}$  is defined as the ratio  $N_{n\bar{n}}(0 < \cos \theta < 0.8)/N_{n\bar{n}}(-0.8 < \cos \theta < 0)$ . The asymmetry  $\alpha_{as}$  is shown in Fig. 6 as a function of the beam energy  $E_b$ . Its average value is  $\alpha_{as} = 1.11 \pm 0.04$ . It is unlikely, but it is also not excluded, that this is an asymmetry of the detector itself. This may be a feature of the  $e^+e^- \rightarrow n\bar{n}$  process with a large momentum imbalance, since asymmetry is not observed in the analysis of other  $e^+e^-$ -annihilation processes.

TABLE I: The beam energy ( $E_b$ ), neutron momentum ( $p$ ), integrated luminosity ( $L$ ), number of selected  $n\bar{n}$  events ( $N_{n\bar{n}}$ ), and measured  $|G_E|/|G_M|$  ratio. The quoted errors for  $|G_E|/|G_M|$  and  $N_{n\bar{n}}$  are statistical and systematic.

N	$E_b$ (MeV)	$p$ (MeV/c)	$L$ (1/pb)	$N_{n\bar{n}}$	$ G_E / G_M $
1	945.5	51	9.38	$882 \pm 41$	$1.321 \pm 0.401 \pm 0.099$
2	950.3	67	9.44	$978 \pm 40$	$1.473 \pm 0.388 \pm 0.184$
3	960.3	86	9.17	$962 \pm 38$	$1.371 \pm 0.332 \pm 0.225$
4	968.8	101	8.78	$909 \pm 38$	$1.122 \pm 0.293 \pm 0.139$
5	970.8	122	5.99	$625 \pm 37$	$0.523 \pm 0.440 \pm 0.203$
6	980.3	133	8.17	$764 \pm 37$	$1.064 \pm 0.337 \pm 0.151$
7	990.4	140	9.40	$811 \pm 39$	$1.352 \pm 0.398 \pm 0.306$
8	1003.5	147	22.5	$1562 \pm 61$	$1.530 \pm 0.340 \pm 0.115$

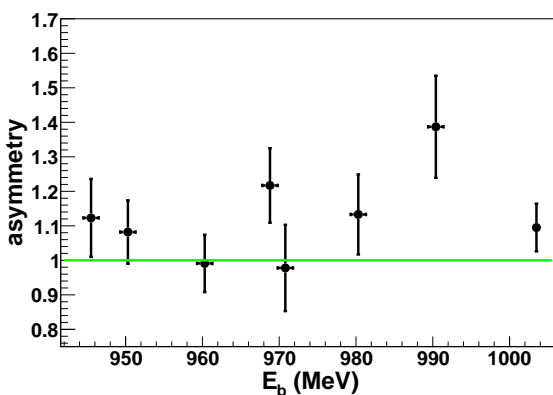


FIG. 6: The right/left asymmetry in the  $\cos\theta$  distribution for data events as a function of the beam energy. The horizontal line corresponds to the case of no asymmetry.

There are also physical reasons for charge asymmetry. It is known that charge asymmetry in the production of fermion pairs (e.g. muons [12]) can reach more than a few percent when taking into account higher order QED corrections. In our case of  $n\bar{n}$  pairs this could be, for example, a process of the type of  $e^+e^- \rightarrow \gamma^*\gamma^* \rightarrow n\bar{n}$ . In Particles Data Group (PDG) Tables [13] there is a tensor state  $f_2(1950)$  decaying into a nucleon-antinucleon pair, which can contribute to the asymmetry. There are no calculations of charge asymmetry for nucleon pairs in the threshold region. But in any case, the observed asymmetry  $\sim 10\%$  looks too large to be due to physical nature. Below in the text, when considering the systematics, we evaluate the influence of asymmetry on the measured value of  $|G_E|/|G_M|$ .

#### IV. MEASUREMENT OF THE NEUTRON $|G_E|/|G_M|$ RATIO

To obtain the  $|G_E|/|G_M|$  value, the data  $\cos\theta$  distribution shown in Fig. 5 is fitted with the following function:

$$F(\cos\theta) = N(H_M(\cos\theta) + \frac{1}{\gamma^2} |\frac{G_E}{G_M}|^2 H_E(\cos\theta)), \quad (6)$$

where  $H_M$  and  $H_E$  are the  $\cos\theta$  distributions for selected simulated  $n\bar{n}$  events generated with the angular distributions  $1 + \cos^2\theta$  and  $\sin^2\theta$  (see Eq. (2)), respectively. The shape  $H_M$  and  $H_E$  distributions differ from the generated initial distributions due to nonuniform detection efficiency (see Fig. 4), the finite  $\theta$  resolution ( $\sigma_\theta \approx 8^\circ$ ), and the radiative corrections. The number of events  $N$  and  $|G_E|/|G_M|$  are free fit parameters in Eq. (6). The result of the fit is shown in Fig. 5. The fitting procedure is performed in each of 8 experimental energy points in Table I.

To estimate systematic uncertainties, we vary parameters that can influence the shape of the  $\cos\theta$  distribution. Removing the condition of no charged tracks in an event results in a shift in  $|G_E|/|G_M|$  by an average of 0.05. Relaxing the condition on the transverse EMC energy profile changes  $|G_E|/|G_M|$  by approximately 0.1. Variations of the time position of the beam background peak within 0.5 ns lead to a significant effect at  $E_b > 700$  MeV. The change in  $|G_E|/|G_M|$  is about 0.08. To check the influence of the asymmetry in the  $\cos\theta$  distribution, we fit the  $|\cos\theta|$  distribution. The obtained shift in  $|G_E|/|G_M|$  is about 0.06 at  $E_b < 700$  MeV and about 0.11 at  $E_b > 700$  MeV. The systematic uncertainties from all sources are combined quadratically. The obtained  $|G_E|/|G_M|$  values with statistical and systematic uncertainties are listed in Table I.

The measured values of the  $|G_E|/|G_M|$  ratio versus the beam energy are shown in Fig. 7. The  $|G_E|/|G_M|$  dependence on the antineutron momentum is presented in Fig. 8. Existing data of experiments [2, 6] are also shown in both plots for comparison. We conclude that the measured  $|G_E|/|G_M|$  values lie mainly within the range 1.0–1.5. The obtained results are in moderate agreement with the calculations of Ref. [14].

#### V. SUMMARY

In the experiment to study the  $e^+e^- \rightarrow n\bar{n}$  process, the ratio  $|G_E|/|G_M|$  of the neutron electric and magnetic form factors in timelike region has been measured. The experiment was carried out at the VEPP-2000  $e^+e^-$  collider with the SND detector at 8 energy points in the

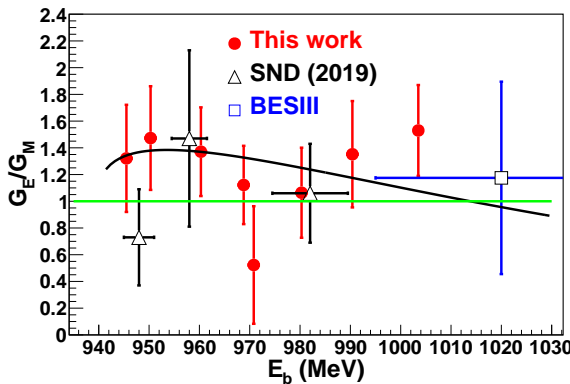


FIG. 7: The dependence of the measured  $|G_E|/|G_M|$  ratio (solid circles) on the beam energy. Data of earlier measurements SND [2] (empty triangle) and BESIII [6] (solid stars) are shown as well. The horizontal line corresponds to the threshold value  $|G_E|/|G_M| = 1$ . Solid curve is the prediction from Ref. [14].

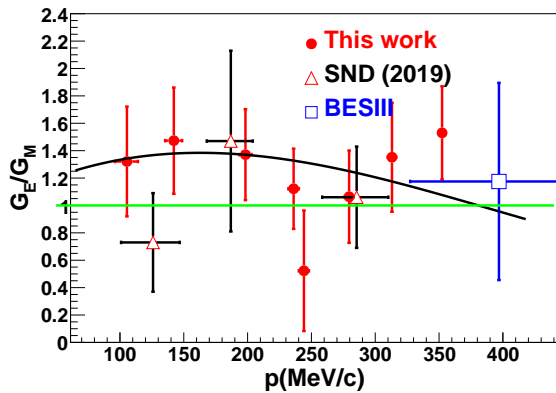


FIG. 8: The dependence of the measured  $|G_E|/|G_M|$  ratio (solid circles) on the antineutron momentum. Solid curve is the prediction from Ref. [14].

beam energy range from 945 to 1000 MeV. The measured value of  $|G_E|/|G_M|$  lies within 1.0–1.5. The statistical accuracy of measurements is about 0.30, while the systematic uncertainties are in the range 0.1–0.3. The obtained data do not contradict earlier measurements of SND [2] and BESIII [6], as well as the theoretical calculation [14].

---

[1] A. Antonelli *et al.* (FENICE Collaboration), Nucl. Phys. **B17**, 3 (1998). [https://doi.org/10.1016/S0550-3213\(98\)00083-2](https://doi.org/10.1016/S0550-3213(98)00083-2)

[2] M. N. Achasov *et al.* (SND Collaboration), Eur. Phys. J. C (2022;82:761). <http://doi.org/10.1140/epjc/s10052-022-10696-0>, e-Print:2206.13047[hep-ex]

[3] M. N. Achasov *et al.* (SND Collaboration), Phys. Part Nucl. **54** No.4, 624 (2023)

[4] M. N. Achasov *et al.* (SND Collaboration), Phys. Atomic Nucl. **86** No.6, 1165 (2023). e-Print:2309.05241[hep-ex]

[5] M. N. Achasov *et al.* (SND Collaboration), Phys. Atomic Nucl. **87** No.5, 604 (2024) e-Print:2407.15308[hep-ex]

[6] M. Ablikim *et al.* (BESIII Collaboration), Nat. Phys. **17**, 1200 (2021). <https://doi.org/10.1038/s41567-021-01345-6>

[7] P. Yu. Shatunov *et al.*, Part. Nucl. Lett. **13**, 995 (2016). <http://dx.doi.org/10.1134/S154747711607044X>

[8] M. N. Achasov *et al.* (SND Collaboration), Nucl. Instrum. Meth. A **449**, 125 (2000). [http://dx.doi.org/10.1016/S0168-9002\(99\)01302-9](http://dx.doi.org/10.1016/S0168-9002(99)01302-9)

[9] M. N. Achasov *et al.*, Nucl. Instrum. Meth. A **1056**, 168664 (2023). <http://dx.doi.org/10.1016/j.nima.2023.168664>

[10] A. V. Bozhenok *et al.*, Nucl. Instr. Meth. A **379**, 507 (1996). [http://dx.doi.org/10.1016/0168-9002\(96\)00548-7](http://dx.doi.org/10.1016/0168-9002(96)00548-7)

[11] J. Allison *et al.* (GEANT Collaboration), Nucl. Instr. Meth. A **835**, 186 (2016). <https://doi.org/10.1016/j.nima.2016.06.125>, <https://geant4-data.web.cern.ch/ReleaseNotes/ReleaseNotes4.10.5.html>

[12] B. Adeva *et al.*, Phys. Rev. Lett. **48**, No.2, 1701 (1982). <https://doi.org/10.1103/PhysRevLett.48.1701>

[13] S. Navas *et al.*, (Particle Data Group), Phys. Rev. D **110**, 030001 (2024)

[14] A.I. Milstein and S.G. Salnikov, Phys. Rev. D. **106**, 074012 (2022). e-print 2207.14020[hep-ph]